

Research Article

Open Access

Julien Mathieu Elias Fraïsse* and Daniel Braun

Quantum channel-estimation with particle loss: GHZ versus W states

DOI 10.1515/qmetro-2016-0009

Received October 31, 2016; accepted January 10, 2017

Abstract: We consider quantum channel-estimation for depolarizing channels and phase-flip channels extended by ancilla qubits and fed with a GHZ or W state. After application of the channel one or several qubits can be lost, and we calculate the impact of the loss on the quantum Fisher information that determines the smallest uncertainty with which the parameters of these channels can be estimated.

Keywords: Quantum channel estimation, Quantum Fisher Information, Quantum metrology, Depolarizing channel, Phase-flip channel

PACS: 03.67.-a, 03.67.Lx

1 Introduction

With the rise of quantum information processing the need to precisely characterize quantum devices has become an important practical issue. Contrary to classical bits, qubits have a continuous range of possible pure states, and their phase coherence is crucial for quantum algorithms. Under the influence of the environment, qubits suffer decoherence processes which can manifest themselves not only in a flip of the bit, but also in a loss of phase coherence. If the corresponding error rates are small enough, quantum error-correction can be applied, which, when concatenated, allows one to ultimately perform meaningful quantum computations. For the development of the hardware and optimization of the quantum error correction it is, however, crucial to precisely know the error mechanisms and rates. This amounts to performing a “quantum channel-estimation”. For a single qubit, the set of possible quantum channels and their possible parametrizations

are well known by now [3, 6, 19], and quantum channel-estimation amounts hence to estimating these parameters.

Quantum channel-estimation is therefore very similar to quantum parameter estimation (q-pet), where one tries to estimate the parameters that determine a quantum state. Q-pet is very well developed, starting with work by Helstrom and Holevo in the 1970s and Braunstein and Caves in the 1990s [8–10, 23–25]. This led to the important insight that the smallest possible uncertainty of the estimation of a parameter is fully determined by the parameter-dependence of the quantum state. The quantum Cramér-Rao bound (QCRB) quantifies this smallest uncertainty and generalizes corresponding results from classical statistical analysis from the 1940s [14, 41]. The theoretical framework has been used to analyze the ultimate possible sensitivity of gravitational wave observatories [29], Mach-Zehnder and atomic interferometers [22, 26, 35, 44], measurements of time [9], mass [4, 5], temperature and chemical potential [13, 32, 33, 42], parameters of space-time [1, 7], and many more.

In addition to the optimization over all possible measurements and data analysis schemes that is inherent in the QCRB, quantum channel-estimation allows one to also optimize over the input state. It has long been known that using highly entangled states can enhance the precision of certain measurements beyond what is possible classically [21], even though measurements exist where such enhancements do not need entanglement, or the naturally occurring “entanglement” due to the symmetrization of states of identical particles is enough for improved performance [2, 16, 31].

It is also known that the quantum advantage can break down very rapidly with the smallest amount of decoherence. For example, Markovian decoherence, no matter how small, always leads back to the so-called standard quantum limit of the uncertainty of atomic clocks, when these are operated with a highly entangled GHZ state [27]. From interferometry it is well known that GHZ states are also maximally fragile against loss of qubits: Even the loss of a single one turns the state into a uniform mixture of the original pure components in the Hilbert space of the remaining particles, and hence erases any useful phase in-

*Corresponding Author: Julien Mathieu Elias Fraïsse: Eberhard-Karls-Universität Tübingen, Institut für Theoretische Physik, 72076 Tübingen, Germany, E-mail: julien.fraisse@uni-tuebingen.de

Daniel Braun: Eberhard-Karls-Universität Tübingen, Institut für Theoretische Physik, 72076 Tübingen, Germany

formation [28]. W states are more robust here, as are “entangled coherent states” [46].

One might wonder then, how useful highly entangled states are for measuring decoherence processes themselves. Interestingly, it was found by Fujiwara and Imai that the best estimation of a Pauli quantum channel of a single qudit can be achieved by sourcing a maximally entangled state into the channel extended by just one more qudit [20]. Frey *et al.* studied the depolarizing channel and considered the performance of several extension schemes [17], and Collins and coworkers examined the depolarizing channel and the phase-flip channel fed with mixed states [11, 12].

In the present work we investigate channel estimation for the depolarizing channel and the phase-flip channel, when these channels are extended by using several ancilla qubits. We consider GHZ states and W states as input and investigate the effect of loss of one or several of the qubits, both the original one or the ancillas, on the precision with which the parameters of the channels can be estimated.

2 Quantum estimation of channels

2.1 Channels

Let $\mathcal{B}_1 = \mathcal{B}(\mathcal{H}_1)$ be the space of bounded linear operators acting on a first Hilbert space \mathcal{H}_1 and $\mathcal{B}_2 = \mathcal{B}(\mathcal{H}_2)$ the space of bounded linear operators acting on a second Hilbert space \mathcal{H}_2 . A quantum channel \mathcal{E} is a *completely positive trace preserving* (CPTP) convex-linear map $\mathcal{E} : \mathcal{B}_1 \rightarrow \mathcal{B}_2$ that maps a density matrix (*i.e.* a positive linear operator with trace one) to another density matrix, $\rho \in \mathcal{B}_1 \mapsto \sigma \in \mathcal{B}_2$. The condition of complete positivity means that the channel should be a positive map (*i.e.* maps positive operators to positive ones), but also that the extension $\mathcal{E} \otimes \text{Id}$ of the channel to ancillary Hilbert spaces \mathcal{H} , where it acts by the identity operator, should be a positive map, *i.e.* $(\mathcal{E} \otimes \text{Id})(A) \geq 0$ for any positive operator A in $\mathcal{B}(\mathcal{H}_1 \otimes \mathcal{H})$, the space of bounded operator acting on the bipartite system $\mathcal{H}_1 \otimes \mathcal{H}$ [36]. Trace preservation is defined as $\text{tr}[\mathcal{E}(\rho)] = \text{tr}[\rho]$, and convex linearity as $\mathcal{E}(\sum_i p_i \rho_i) = \sum_i p_i \mathcal{E}(\rho_i)$ for all p_i with $0 \leq p_i \leq 1$ and $\sum_i p_i = 1$. According to Kraus’ theorem, a quantum channel can be represented as

$$\mathcal{E}(\rho) = \sum_i E_i \rho E_i^\dagger, \quad (1)$$

where the Kraus operators $\{E_i\}$ satisfy $\sum_i E_i^\dagger E_i = \mathcal{J}_2$, the identity operator on the target Hilbert space \mathcal{H}_2 [30].

In the following we study the two physically important channels “depolarizing channel” and “phase-flip channel” for a single qubit [36]. The depolarizing channel describes relaxation,

$$\mathcal{E}_{\text{dep}}(\rho) = p \frac{\mathcal{J}}{2} + (1-p)\rho, \quad (2)$$

i.e. the qubit is replaced with probability p (the “depolarization strength”) by the totally mixed state. Its Kraus decomposition is given by

$$\mathcal{E}_{\text{dep}}(\rho) = \sum_{i=1}^4 E_i \rho E_i^\dagger, \quad (3)$$

with the four Kraus operators:

$$E_1 = \sqrt{1 - 3\frac{p}{4}} \mathcal{J}, E_2 = \sqrt{\frac{p}{4}} X, E_3 = \sqrt{\frac{p}{4}} Y, E_4 = \sqrt{\frac{p}{4}} Z,$$

where X, Y and Z are the three Pauli matrices.

The phase-flip channel has the Kraus representation

$$\mathcal{E}_{\text{ph}}(\rho) = \sum_{i=1}^2 F_i \rho F_i^\dagger, \quad (4)$$

with the Kraus operators

$$F_1 = \sqrt{1-p} \mathcal{J}, F_2 = \sqrt{p} Z, \quad (5)$$

i.e. with probability p the phase of the qubit is flipped.

We also define extensions of these channels by the identity to n ancilla qubits, on which the channels act through the identity operation. For the depolarizing channel we have

$$\mathcal{E}_{\text{dep}}^{(n)}(\rho) = (\mathcal{E}_{\text{dep}} \otimes \text{Id} \cdots \otimes \text{Id})(\rho) = \sum_{i=1}^4 \Gamma_i \rho \Gamma_i^\dagger, \quad (6)$$

where the Kraus operators Γ_i of the extended channel are defined as $\Gamma_i = E_i \otimes \mathcal{J}^{\otimes n}$.

Similarly, we extend the phase-flip channel to n ancilla qubits by

$$\mathcal{E}_{\text{ph}}^{(n)}(\rho) = (\mathcal{E}_{\text{ph}} \otimes \text{Id} \cdots \otimes \text{Id})(\rho) = \sum_{i=1}^2 \Lambda_i \rho \Lambda_i^\dagger \quad (7)$$

with the new Kraus operators $\Lambda_i = F_i \otimes \mathcal{J}^{\otimes n}$.

2.2 Quantum parameter estimation

Quantum parameter estimation theory (q-pet) [8, 9, 23, 24] provides a lower bound on the variance of an unbiased estimator $\hat{\theta}_{\text{est}}$ of a parameter θ on which a state $\rho(\theta)$ depends. Its importance arises from the facts that

(i) it is optimized already over all possible measurements (POVM measurements, generalizing projective von Neumann measurements [38]), and all possible data analysis schemes in the form of unbiased estimators (*i.e.* estimators that on the average give back the true value of the parameter); and (ii) the bound is reachable at least asymptotically, in the limit of an infinite number of measurements. This so-called quantum Cramér-Rao bound (QCRB) is given by

$$\text{Var}(\hat{\theta}_{\text{est}}) \geq \frac{1}{M I(\rho(\theta))}, \quad (8)$$

with M the number of independent measurements and $I(\rho(\theta))$ the quantum Fisher information (QFI). In [8] it was shown that $I(\rho(\theta))$ is a geometric measure on how much $\rho(\theta)$ and $\rho(\theta + d\theta)$ differ, where $d\theta$ is an infinitesimal increment of θ . The QCRB thus offers the physically intuitive picture that the parameter θ can be measured the more precisely the more strongly the state $\rho(\theta)$ depends on it (see below for a precise definition). The geometric measure is given by the Bures-distance,

$$d_B(\rho, \sigma)^2 \equiv 2 \left(1 - \sqrt{F(\rho, \sigma)} \right), \quad (9)$$

where the fidelity $F(\rho, \sigma)$ is defined as $F(\rho, \sigma) = \|\rho^{1/2} \sigma^{1/2}\|_1^2$, and $\|A\|_1 \equiv \text{tr} \sqrt{AA^\dagger}$ denotes the trace norm [34]. With this, $I(\rho(\theta)) = 4 d_B(\rho(\theta), \rho(\theta + d\theta))^2 / d\theta^2$ [8]. The Bures-distance is in general difficult to calculate for mixed states, but for pure states $\rho(\theta) = |\psi(\theta)\rangle\langle\psi(\theta)|$, the QFI reduces to the overlap of the derivative of the state, $|\partial_\theta \psi(\theta)\rangle$, with itself and the original state, $I(\rho(\theta)) = 4(\langle \partial_\theta \psi(\theta) | \partial_\theta \psi(\theta) \rangle - |\langle \partial_\theta \psi(\theta) | \psi(\theta) \rangle|^2)$ [37].

When the state is not pure we can still give a closed formula by using the spectral representation of the state. For

$$\rho(\theta) = \sum_{i=1}^d p_i |\psi_i\rangle\langle\psi_i|, \quad (10)$$

the QFI can be written as

$$I(\rho(\theta)) = \sum_{\substack{i=1 \\ p_i \neq 0}}^d \frac{(\partial_\theta p_i)^2}{p_i} + \sum_{\substack{i,j=1 \\ p_i + p_j \neq 0}}^d \frac{2(p_i - p_j)^2}{p_i + p_j} |\langle \psi_j | \partial_\theta \psi_i \rangle|^2,$$

where the first term is called classical contribution and the second quantum contribution.

The QFI obeys the “monotonicity property” under θ -independent channels \mathcal{E}

$$I(\mathcal{E}(\rho(\theta))) \leq I(\rho(\theta)), \quad (11)$$

with equality for unitary channels \mathcal{U} , defined by $\mathcal{U}(\rho) = U\rho U^\dagger$ [39] with U unitary. The QFI has also the property of convexity, meaning that for two density matrices $\rho(\theta)$ and $\sigma(\theta)$ and $0 \leq \lambda \leq 1$ we have [18]

$$I(\lambda\rho(\theta) + (1 - \lambda)\sigma(\theta)) \leq \lambda I(\rho(\theta)) + (1 - \lambda) I(\sigma(\theta)). \quad (12)$$

A last useful property of the QFI is the additivity:

$$I(\rho(\theta) \otimes \sigma(\theta)) = I(\rho(\theta)) + I(\sigma(\theta)). \quad (13)$$

For a state that depends on several parameters $\theta = (\theta_1, \dots, \theta_n)$, the QCRB generalizes to an inequality for the co-variance matrix of the estimators of the θ_i , with a lower bound given by the inverse of the quantum Fisher information matrix. In contrast to the single parameter case, this inequality can in general not be saturated (see [43] and references therein) but one can still try to optimize the trade-off in joint estimation (see [15, 45] for estimation of phase and noise simultaneously).

2.3 Quantum channel-estimation

2.3.1 General considerations

We consider channels \mathcal{E}_θ depending on a scalar parameter θ , and perfectly known initial states ρ independent of θ . After the evolution of ρ through the channel, we obtain a state parametrized by θ with QFI

$$I(\rho(\theta)) = I(\mathcal{E}_\theta(\rho)) \quad (14)$$

that can still be optimized over ρ . Due to the convexity of the QFI, its maximal value can be achieved with a pure state. The fact that a quantum channel is a completely positive map allows one to extend it to a larger Hilbert space by acting with an arbitrary quantum channel \mathcal{A} on the Hilbert space of the ancilla,

$$\mathcal{E}_\theta^{\text{ext}, \mathcal{A}} = \mathcal{E}_\theta \otimes \mathcal{A}. \quad (15)$$

According to an argument by Fujiwara [18], the largest QFI with a parameter independent \mathcal{A} can be achieved already by choosing for \mathcal{A} the identity channel in the ancillary Hilbert space: Since $\mathcal{E}_\theta \otimes \mathcal{A}$ can be decomposed as $(\text{Id} \otimes \mathcal{A})(\mathcal{E}_\theta \otimes \text{Id})$, monotonicity of the QFI implies that the best choice for $(\text{Id} \otimes \mathcal{A})$ is a unitary channel, which is the case when \mathcal{A} is a unitary channel. The simplest solution consists in taking the identity channel and thus, in the following, when we refer to extensions, we always mean an extension *by the identity channel in the Hilbert space of the ancilla*.

2.3.2 Estimation of depolarizing and phase-flip channels

For both depolarizing and phase-flip channels, the parameter to be estimated is p . To avoid cumbersome notation,

we omit the dependence on p in the states, the channels, and the QFI.

For the depolarizing channel acting on one qubit, all states related by a p -independent unitary transformation U give rise to the same QFI, as

$$\mathcal{E}_{\text{dep}}(U\rho U^\dagger) = U\mathcal{E}_{\text{dep}}(\rho)U^\dagger, \quad (16)$$

coupled to the fact that the QFI is invariant under parameter-independent unitary transformations of the state. For the phase-flip channel, the initial state and in particular the orientation of its Bloch vector matters, as in general for an arbitrary unitary U

$$\mathcal{E}_{\text{ph}}(U\rho U^\dagger) \neq U\mathcal{E}_{\text{ph}}(\rho)U^\dagger. \quad (17)$$

2.4 Known results

In [20] Fujiwara and Imai investigated the problem of estimating generalized Pauli channels acting on qudits — *i.e.* systems with a d -dimensional Hilbert space and, in general, $d^2 - 1$ parameters $\{p_i\}_{1 \leq i \leq d^2-1}$ to estimate. The authors were interested in the optimal protocol for estimating these parameters when one uses the channel m times. They showed that the optimal protocol (in terms of the QFI matrix) consists in making m independent estimations of the channel extended to a single ancillary qudit with the same dimension of Hilbert space and to input a pure, maximally entangled state $|\psi_d^{\text{m.e.}}\rangle$

$$|\psi_d^{\text{m.e.}}\rangle = \sum_{i=1}^d \frac{1}{\sqrt{d}} |u_i\rangle \otimes |v_i\rangle \quad (18)$$

with $\{|u_i\rangle\}$ and $\{|v_i\rangle\}$ two orthonormal bases ($\langle u_i | u_j \rangle = \langle v_i | v_j \rangle = \delta_{ij}$).

In the specific case of the qubit ($d = 2$), the Pauli channels are the channels constructed with Pauli matrices as Kraus operators,

$$\mathcal{E}_{\text{Pauli}}(\rho) = (1 - p_1 - p_2 - p_3)\rho + p_1 X\rho X + p_2 Y\rho Y + p_3 Z\rho Z, \quad (19)$$

i.e. the estimation of Pauli channels for qubits is in general a 3-parameter estimation problem. It reduces to the estimation of the depolarizing channel by setting $p_1 = p_2 = p_3 = p/4$, while the phase-flip channel corresponds to the case $p_1 = p_2 = 0$. The well-known four Bell states

$$|\phi_\pm\rangle = \frac{|00\rangle \pm |11\rangle}{\sqrt{2}}, \quad |\varphi_\pm\rangle = \frac{|01\rangle \pm |10\rangle}{\sqrt{2}}, \quad (20)$$

are special cases of maximally entangled states for $d = 2$, and thus achieve the optimal QFI for the estimation of

$\{p_1, p_2, p_3\}$, the three parameters attached to Pauli channels for qubits.

Frey *et al.* analyzed the depolarizing channel acting on qudits using different extension schemes, including sequential protocols, where the same probe undergoes m times the channel before any measurement is done [17]. A fair figure of merit for the comparison is then the QFI *per channel application*. The schemes studied were (i) the non-extended original channel \mathcal{E}_{dep} ; (ii) the channel extended by the identity in an ancillary q -dimensional Hilbert space, $\mathcal{E}_{\text{dep}} \otimes \text{Id}$; (iii) the original channel applied in parallel to two different qudits, $\mathcal{E}_{\text{dep}} \otimes \mathcal{E}_{\text{dep}}$; (iv) the channel extended by a known depolarizing channel with depolarizing strength η , $\mathcal{E}_{\text{dep},p} \otimes \mathcal{E}_{\text{dep},\eta}$, where the subscripts p and η denote the respective depolarizing strengths, and (v) the m times iterated use of the channels in schemes (i, ii, iii). Pure input states were considered, with a maximally entangled state in all the schemes with more than one qudit, and in addition partially entangled states in scheme (ii).

From the work of Fujiwara and Imai [20] it is clear that the best scheme is (ii) with a maximally entangled state as input. It also turns out that the multiple use of the probes is useless in the sense that the QFI per channel use is always smaller or equal in the sequential schemes than in the non-sequential ones. Depending on the dimension d of the Hilbert space of the qudit, and on the depolarization strength p , the simple scheme (i) or the double use of the channel (iii) fair better. Partially entangled pure states in scheme (ii) lead to a QFI lying between the one of the optimal scheme and the one of the simple scheme. When the additional depolarization η in scheme (iv) is too large, it becomes more efficient to just use the simple channel or the doubled channel.

Collins considered mixed states for the estimation of the phase-flip channel [11] and in [12] Collins and Stephens did the same for the depolarizing channel. They studied sequential protocols, where there is just one qubit available on which the channel is applied m times, and also parallel or multi-qubit protocols. For these they investigated the effect of correlation among more than two qubits on the efficiency. Again the figure of merit was the QFI per channel application, and the results were compared to the protocol with just one channel and one qubit (SQSC protocol). Depending on purity and depolarization strength, both sequential and correlated protocols can outperform the SQSC protocol. Especially for extremely small purity of qubits, adding more ancillas in the correlated protocol increases the QFI, and the correlated protocol proves to be better than the sequential one.

Fujiwara and Imai’s optimal metrological strategy for the estimation of Pauli channels implies that no gain in the QFI is to be expected by extending the channels to ancillary Hilbert spaces with a dimension greater than the one of the original space. Nevertheless, such extensions still have an interest in the case where one faces the loss of particles. In this non-ideal situation, adding more ancillas to the probe may eventually prove useful. We thus study channel estimation with W and GHZ states composed of $n+1$ qubits (the original probe and n ancillas) as input, and investigate in particular the robustness of these schemes under loss of particles.

2.5 Benchmark

We first calculate two benchmarks for the QFI: The first one, $I_{\mathcal{E}_\theta}^{\text{opt}}$, corresponds to the optimal case identified by Fujiwara and Imai [20], namely extending the quantum channel by the identity to a second qubit and feeding it with a maximally entangled state: $I_{\mathcal{E}_\theta}^{\text{opt}} = I((\mathcal{E}_\theta \otimes \text{Id})(|\psi^{\text{m.e.}}\rangle\langle\psi^{\text{m.e.}}|))$.

The second one, $I_{\mathcal{E}_\theta}^{\text{sep}}$, is given by directly estimating the parameter of the channel acting on a single qubit and optimizing over all pure input states: $I_{\mathcal{E}_\theta}^{\text{sep}} = \max_{|\psi\rangle\langle\psi|} I(\mathcal{E}_\theta(|\psi\rangle\langle\psi|))$. This latter scheme is, in terms of QFI, equivalent to the case where one uses an extended channel (of the form (6) or (7), or in fact an arbitrary θ -independent extension acting separately on the original system and the ancillas) but inputs a separable state. Indeed, due to the additivity of the QFI we have

$$\begin{aligned} I((\mathcal{E}_\theta \otimes \mathcal{A})(\rho \otimes \sigma)) &= I(\mathcal{E}_\theta(\rho) \otimes \mathcal{A}(\sigma)) \\ &= I(\mathcal{E}_\theta(\rho)) + I(\mathcal{A}(\sigma)) \\ &= I(\mathcal{E}_\theta(\rho)), \end{aligned}$$

since the state $\mathcal{A}(\sigma)$ is θ -independent. Thus we refer to this case as “separable strategy”.

2.5.1 Depolarizing channel

In the non-extended case, the QFI for the depolarizing channel depends only on the purity of the input state. When starting with a pure state of a single qubit we obtain for the QFI

$$I_{\text{dep}}^{\text{sep}} = \frac{1}{p(2-p)}. \quad (21)$$

The optimal strategy leads to

$$I_{\text{dep}}^{\text{opt}} = \frac{3}{p(4-3p)}. \quad (22)$$

In more detail, the depolarizing channel transforms a Bell state as

$$\mathcal{E}_{\text{dep}}^{(1)}(\phi_+) = (1 - 3\frac{p}{4})\phi_+ + \frac{p}{4}(\phi_- + \varphi_+ + \varphi_-), \quad (23)$$

where $\phi_\pm = |\phi_\pm\rangle\langle\phi_\pm|$, $\varphi_\pm = |\varphi_\pm\rangle\langle\varphi_\pm|$. I.e. the channel creates a mixture between ϕ_+ and a state orthogonal to it, $\phi_- + \varphi_+ + \varphi_-$ [40]. This makes the scheme more sensitive to the value of the parameter than for the separable strategy. With the two benchmarks (21,22) we can check whether extending the channel still leads to an improvement compared to the separable strategy when qubits can be lost by comparing the QFI to $I_{\text{dep}}^{\text{sep}}$, but also how far the QFI is stable against losing qubits compared to the optimal strategy, a property that we call “robustness”.

2.5.2 Phase-flip channel

The case of the phase-flip channel is slightly different. Due to the anisotropy of the channel, the QFI of the non-extended strategy depends on the polar angle θ of the Bloch vector. The QFI is optimized by states $|\psi_{xy}\rangle = (|0\rangle + e^{-i\varphi}|1\rangle)/\sqrt{2}$ (i.e. $\theta = \pi/2$), and has the value

$$I_{\text{ph}}^{\text{sep},xy} = \frac{1}{p(1-p)}. \quad (24)$$

The optimal strategy leads to

$$I_{\text{ph}}^{\text{opt}} = \frac{1}{p(1-p)}, \quad (25)$$

which is equal to $I_{\text{ph}}^{\text{sep},xy} \equiv I_{\text{ph}}^{\text{sep}}$, showing that the state $|\psi_{xy}\rangle$ is optimal for the separable strategy (since $I_{\text{ph}}^{\text{opt}}$ is an upper bound for the QFI of the separable strategy, and this upper bound is reached with the states $|\psi_{xy}\rangle$). For ideal phase-flip channels the extension is thus useless, in the sense that we can achieve the same sensitivity with separable states or entangled ones ¹. Here both benchmarks (24) and (25) are equal. Hence there is no metrological interest in adding any ancillas. Nevertheless, from a mathematical perspective it is still interesting to see the effect of adding ancillas and losing a fraction of them.

¹ This is a well known fact. Indeed, in [20](part 4.) the authors emphasized that when estimating the parameter of a Pauli channel lying on the boundaries of the tetrahedron of the simplex representing the different Pauli channels, non-maximally entangled states may be as efficient as maximally entangled ones. They also noticed that for the phase damping channel and for the bit flip channel a separable state is already optimal.

2.6 Used input states

For feeding our extended channels we consider two kinds of entangled states, GHZ states and W states. The GHZ (Greenberger-Horne-Zeilinger) state for $n + 1$ qubits is defined as

$$|\psi^{\text{GHZ-}n}\rangle = \frac{1}{\sqrt{2}}(|0, 0_n\rangle + |1, \mathbb{1}_n\rangle), \quad (26)$$

with $|0, 0_n\rangle = |0\rangle_1 \otimes |0\rangle_2 \otimes \cdots \otimes |0\rangle_{n+1}$, $|0, \mathbb{1}_n\rangle = |0\rangle_1 \otimes |1\rangle_2 \otimes \cdots \otimes |1\rangle_{n+1}$, $|1, 0_n\rangle = |1\rangle_1 \otimes |0\rangle_2 \otimes \cdots \otimes |0\rangle_{n+1}$ and $|1, \mathbb{1}_n\rangle = |1\rangle_1 \otimes |1\rangle_2 \otimes \cdots \otimes |1\rangle_{n+1}$. Here and in the following, the first Hilbert space is the one of the probe and all the others are for ancillas, and we take $n \geq 1$. When $n = 1$, the GHZ state $|\psi^{\text{GHZ-}1}\rangle$ is equal to the Bell state $|\phi_+\rangle$. GHZ states are very prone to decoherence, in the sense that if even a single qubit is lost (traced out), we end up with a mixed non-entangled state (see eq.(41) below). We define the density matrix $\rho^{\text{GHZ-}n} = |\psi^{\text{GHZ-}n}\rangle\langle\psi^{\text{GHZ-}n}|$.

The W state for $n + 1$ qubits, W- n for short, is defined as

$$|\psi^{\text{W-}n}\rangle = \frac{1}{\sqrt{n+1}} \sum_{i=1}^{n+1} |1_i\rangle, \quad (27)$$

with $|1_i\rangle = |0\rangle_1 \otimes \cdots \otimes |0\rangle_{i-1} \otimes |1\rangle_i \otimes |0\rangle_{i+1} \otimes \cdots \otimes |0\rangle_{n+1}$, $\forall i \in \{1, \dots, n+1\}$, i.e. it corresponds to a single excitation distributed evenly over all qubits. The case $n = 1$ gives also a Bell state: $|\psi^{\text{W-}1}\rangle = |\phi_+\rangle$. We also define $\rho^{\text{W-}n} = |\psi^{\text{W-}n}\rangle\langle\psi^{\text{W-}n}|$.

3 Estimation of the ideal quantum channels

We start with the situation where no qubits are lost, and determine the QFI for both GHZ and W states for the two channels that we are interested in.

3.1 Depolarizing channel

3.1.1 GHZ states

For the depolarizing channel acting on the GHZ state, we define

$$\rho_{\text{dep}}^{\text{GHZ-}n} \equiv \mathcal{E}_{\text{dep}}^{(n)}(\rho^{\text{GHZ-}n}) \quad (28)$$

$$\begin{aligned} &= \frac{2-p}{4} (|0, 0_n\rangle\langle 0, 0_n| + |1, \mathbb{1}_n\rangle\langle 1, \mathbb{1}_n|) \\ &+ \frac{1-p}{2} (|1, \mathbb{1}_n\rangle\langle 0, 0_n| + |0, 0_n\rangle\langle 1, \mathbb{1}_n|) \\ &+ \frac{p}{4} (|1, 0_n\rangle\langle 1, 0_n| + |0, \mathbb{1}_n\rangle\langle 0, \mathbb{1}_n|). \quad (29) \end{aligned}$$

The density matrix has rank four for $n \geq 1$ (while for $n = 0$ it has rank 2), but eigenvalues and eigenvectors are still found easily,

$$\begin{cases} \sigma_1^{\text{dep}} = \frac{p}{4}, \sigma_2^{\text{dep}} = \frac{p}{4}, \sigma_3^{\text{dep}} = 1 - \frac{3p}{4}, \sigma_4^{\text{dep}} = \frac{p}{4} \\ |s_1^{\text{dep}}\rangle = |0, \mathbb{1}_n\rangle, |s_2^{\text{dep}}\rangle = |1, 0_n\rangle, \\ |s_3^{\text{dep}}\rangle = \frac{1}{\sqrt{2}} (|0, 0_n\rangle + |1, \mathbb{1}_n\rangle), \\ |s_4^{\text{dep}}\rangle = \frac{1}{\sqrt{2}} (|0, 0_n\rangle - |1, \mathbb{1}_n\rangle). \end{cases}$$

The eigenvectors are independent of p , and the QFI reduces to its classical part,

$$I_{\text{dep}}^{\text{GHZ-}n} = \frac{3}{p(4-3p)} = I_{\text{dep}}^{\text{opt}}. \quad (30)$$

The QFI is independent of the number of ancillas for $n \geq 1$ and equals the QFI corresponding to the optimal case.

3.1.2 W states

For the depolarizing channel and the W states we have

$$\begin{aligned} \rho_{\text{dep}}^{\text{W-}n} &\equiv \mathcal{E}_{\text{dep}}^{(n)}(\rho^{\text{W-}n}) \\ &= \frac{p}{2(n+1)} \left(|0, 0_n\rangle\langle 0, 0_n| + \sum_{i=2}^{n+1} |1, 1_i\rangle\langle 1, 1_i| \right. \\ &+ \sum_{\substack{i,j=2 \\ i \neq j}}^{n+1} |1, 1_i\rangle\langle 1, 1_j| \left. \right) + \frac{2-p}{2(n+1)} \left(\sum_{i=1}^{n+1} |1_i\rangle\langle 1_i| \right. \\ &+ \sum_{\substack{i,j=2 \\ i \neq j}}^{n+1} |1_i\rangle\langle 1_j| \left. \right) + \frac{1-p}{n+1} \sum_{i=2}^{n+1} (|1_i\rangle\langle 1_1| + |1_1\rangle\langle 1_i|), \end{aligned}$$

with $|1, 1_i\rangle = |1\rangle_1 \otimes |0\rangle_2 \otimes \cdots \otimes |0\rangle_{i-1} \otimes |1\rangle_i \otimes |0\rangle_{i+1} \otimes \cdots \otimes |0\rangle_{n+1}$, $\forall i \in \{2, \dots, n+1\}$. The matrix representation in the computational basis has a block structure whose blocks are studied in the appendix, with three non-zero blocks:

- a first trivial 1×1 block composed by the eigenvalue $\frac{p}{2(n+1)}$.
- a second block $G^{(n)}(a)$ with $a = \frac{p}{2(n+1)}$.

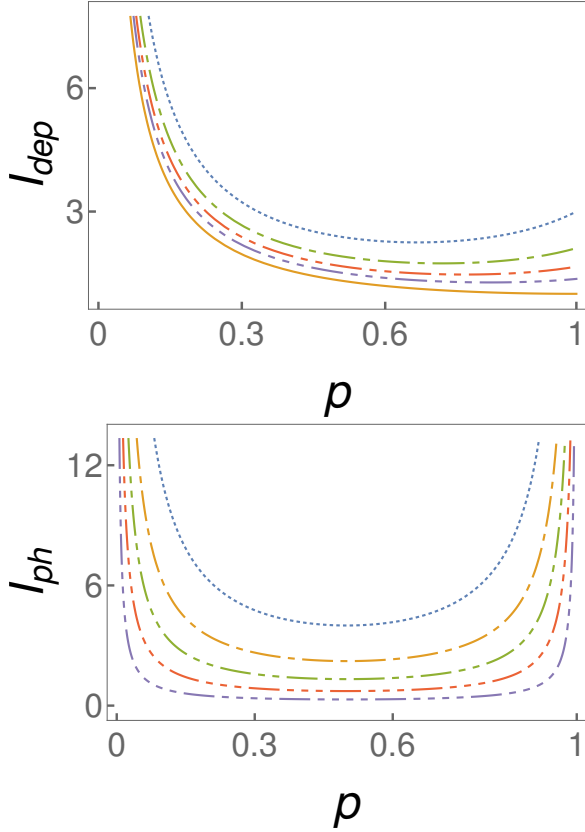


Figure 1: QFI with no loss of qubits. Top plot (depolarizing channel): dotted line: GHZ (optimal strategy); 1-dash line: W-5; 2-dash line: W-10; 3-dash line: W-20; full line: separable state. Bottom plot (phase-flip channel): dotted line: GHZ (optimal separable scheme); 1-dash line: W-5; 2-dash line: W-10; 3-dash line: W-20; 4-dash line: W-50.

- a third block $K^{(n+1)}(a, b, a)$ with $a = \frac{2-p}{2(n+1)}$ and $b = \frac{1-p}{n+1}$.

This leads to the QFI

$$I_{\text{dep}}^{W-n} = \frac{1}{p(2-p)} \frac{(3p - 4(1+n(n+4)))/(1+n)^2}{(3p-4)}. \quad (31)$$

Even if this analysis is restricted to $n \geq 1$, the eq.(31) for $n = 0$ gives the correct QFI. We notice that I_{dep}^{W-n} decreases as function of n , *i.e.* adding ancillas reduces the efficiency of the scheme (see top plot in Fig. 1 or bottom plot in Fig. 2). When we go to an infinite number of ancillas,

$$I_{\text{dep}}^{W-n} \xrightarrow{n \rightarrow \infty} \frac{1}{p(2-p)} = I_{\text{dep}}^{\text{sep}}, \quad (32)$$

i.e. we come back to the case without ancilla.

3.2 Phase-flip channel

3.2.1 GHZ states

Let $\rho_{\text{ph}}^{\text{GHZ}-n} = \mathcal{E}_{\text{ph}}^{(n)}(\rho^{\text{GHZ}-n})$. Applying the Kraus operators, one obtains immediately

$$\rho_{\text{ph}}^{\text{GHZ}-n} = \frac{1}{2} (|0, 0_n\rangle\langle 0, 0_n| + |1, 1_n\rangle\langle 1, 1_n|) + \frac{1-2p}{2} (|1, 1_n\rangle\langle 0, 0_n| + |0, 0_n\rangle\langle 1, 1_n|). \quad (33)$$

The QFI for p , $I_{\text{ph}}^{\text{GHZ}-n}$, is easily found as the operator has rank two. The eigenvalues σ_i^{ph} and eigenvectors $|s_i^{\text{ph}}\rangle$ of $\rho_{\text{ph}}^{\text{GHZ}-n}$ are

$$\begin{cases} \sigma_1^{\text{ph}} = p & , & \sigma_2^{\text{ph}} = 1-p \\ |s_1^{\text{ph}}\rangle = \frac{1}{\sqrt{2}} (|0, 0_n\rangle - |1, 1_n\rangle) & , & |s_2^{\text{ph}}\rangle = \frac{1}{\sqrt{2}} (|0, 0_n\rangle + |1, 1_n\rangle) . \end{cases} \quad (34)$$

The eigenvectors are independent of p , which means that the QFI has just the (classical) contribution from the eigenvalues,

$$I_{\text{ph}}^{\text{GHZ}-n} = \frac{1}{p(1-p)} = I_{\text{ph}}^{\text{opt}}. \quad (35)$$

We see that the QFI for a $(n+1)$ -qubit GHZ state used to estimate a phase-flip channel is independent of the number of ancillas and is equal to the optimal QFI achieved by using either a separable state or a Bell state (but requires more resources in terms of qubits).

3.2.2 W states

The state after acting with the phase-flip channel on the W states, $\rho_{\text{ph}}^{W-n} \equiv \mathcal{E}_{\text{ph}}^{(n)}(\rho^{W-n})$, is given by

$$\rho_{\text{ph}}^{W-n} = \frac{1}{n+1} \left(\sum_{i=1}^{n+1} |1_i\rangle\langle 1_i| + \sum_{\substack{i,j=2 \\ i \neq j}}^{n+1} |1_i\rangle\langle 1_j| \right) + \frac{1-2p}{n+1} \left(\sum_{i=2}^{n+1} (|1_1\rangle\langle 1_i| + |1_i\rangle\langle 1_1|) \right). \quad (36)$$

The matrix representation of this state in the computational basis admits a direct sum decomposition (block structure of the matrix) with a single non-zero block, of the general form $K^{(n+1)}(a, b, a)$, where $a = \frac{1}{n+1}$ and $b = \frac{1-2p}{n+1}$.

Using eq.(62) and the normalized version of eq.(63) we can compute the QFI,

$$I_{\text{ph}}^{W-n} = \frac{4n}{(1+n)^2} \frac{1}{p(1-p)} = \frac{4n}{(1+n)^2} I_{\text{ph}}^{\text{opt}}. \quad (37)$$

This result shows that the QFI decreases with increasing number of ancillas in the W state (see bottom plot in Fig. 1 or bottom plot in Fig. 3): In agreement with the known result on optimality, the prefactor $f(n) = \frac{4n}{(1+n)^2}$ satisfies $f(n) \leq 1$ for $n \geq 1$. When n goes to infinity, $f(n)$ tends to zero, leading to vanishing QFI. Even though our analysis is restricted to $n \geq 1$, for $n = 0$ the W state reduces to $|1\rangle$ which has vanishing QFI such that eq.(37) is still correct.

In Fig. 1 we plot the QFI for depolarizing and phase-flip channel as a function of p when no qubits are lost. We see that the GHZ states gives the highest QFI (we do not have to specify the number of ancillas in the GHZ states since it does not change the QFI). For the W states we observe the decrease of the QFI when increasing the number of ancillas, and the convergence either to the performance of the separable strategy for the depolarizing channel, or to zero for the phase-flip channel.

4 Losing particles

In the section 3 we looked at the QFI for GHZ and W states in the ideal situation of no particle loss in order to check how far we are from the optimal case. We now investigate the effect of losing one particle.

4.1 General considerations

Consider a general extended quantum channel $\mathcal{E}_{\text{ext}} = \mathcal{E}_P \otimes \text{Id}_A$ acting on ρ as

$$\mathcal{E}_{\text{ext}}(\rho) = \sum_k E_k \rho E_k^\dagger = \sum_k (F_k \otimes J_A) \rho (F_k^\dagger \otimes J_A). \quad (38)$$

We use subscripts P and A for probe (the first system) and ancilla, respectively.

We model the loss of one of the systems by tracing it out *after* applying the channel. Physically it means that the state undergoes properly the channel, and that after this and before the measurement, one of the systems is lost. We denote the state which underwent the channel evolution \mathcal{E}_{ext} and then the loss of the probe as $\rho_A^{\mathcal{E}_{\text{ext}}}$. Direct calculation shows that in all generality

$$\rho_A^{\mathcal{E}_{\text{ext}}} \equiv \text{Tr}_P [\mathcal{E}_{\text{ext}}(\rho)] = \text{Tr}_P [\rho], \quad (39)$$

the reduced initial state of the ancilla. In this case there is nothing left to estimate: we cannot get any information on the extended channel by measuring only the ancilla.

If it is the ancilla that is lost after the application of the extended channel on the initial state we have

$$\rho_P^{\mathcal{E}_{\text{ext}}} \equiv \text{Tr}_A [\mathcal{E}_{\text{ext}}(\rho)] = \mathcal{E}_P(\text{Tr}_A [\rho]). \quad (40)$$

In this case, losing the ancilla after extending the channel is equivalent to starting with the non-extended channel acting on the reduced state of the probe. Losing the probe after applying the channel, or starting with an initial state which already suffered the loss of the probe is hence equivalent. From this point of view, our subsequent study amounts to considering new initials states.

4.2 Depolarizing channel

We start the study of the effect of the loss of an ancilla by the depolarizing channel.

4.2.1 GHZ states

When tracing out a qubit from the GHZ state we end up with the mixed state

$$\text{Tr}_1 [\rho^{\text{GHZ-}n}] = \rho_1^{\text{GHZ-}n} = \left(|0, 0_{n-1}\rangle\langle 0, 0_{n-1}| + |1, 1_{n-1}\rangle\langle 1, 1_{n-1}| \right) / 2. \quad (41)$$

We are interested in the QFI $I_{\text{dep},1}^{\text{GHZ-}n}$ of the state $\rho_{\text{dep},1}^{\text{GHZ-}n} \equiv \text{Tr}_1 [\mathcal{E}_{\text{dep}}^{(n)}(\rho^{\text{GHZ-}n})]$. The subscript "1" on the states, on the trace, and on the QFI indicates that we lost *one* ancilla. In virtue of eq.(40) we can also write the state $\rho_{\text{dep},1}^{\text{GHZ-}n}$ as

$$\begin{aligned} \rho_{\text{dep},1}^{\text{GHZ-}n} &= \mathcal{E}_{\text{dep}}^{(n-1)}(\text{Tr}_1 [\rho^{\text{GHZ-}n}]) \\ &= \frac{2-p}{4} (|0, 0_{n-1}\rangle\langle 0, 0_{n-1}| + |1, 1_{n-1}\rangle\langle 1, 1_{n-1}|) \\ &\quad + \frac{p}{4} (|1, 0_{n-1}\rangle\langle 1, 0_{n-1}| + |0, 1_{n-1}\rangle\langle 0, 1_{n-1}|). \end{aligned} \quad (42)$$

For $n = 1$ the state has only rank two, and is actually the totally mixed state of one qubit, *which is a stationary state of the depolarizing channel and thus leads to a vanishing QFI*,

$$I_{\text{dep},1}^{\text{GHZ-}1} = 0. \quad (44)$$

From eq.(43) we obtain directly the QFI for $n > 1$,

$$I_{\text{dep},1}^{\text{GHZ-}n} = \frac{1}{p(2-p)}, \quad (45)$$

which is the same QFI as for the non-extended channel applied to a pure state, $I_{\text{dep}}^{\text{sep}}$. This means that instead of starting with a pure state of a single qubit, we can also start with the mixed state (41) and use the extended channel.

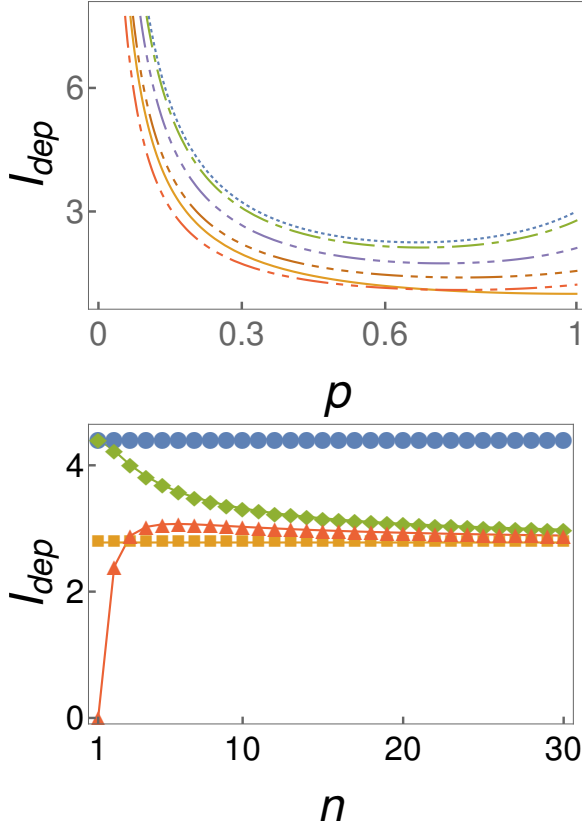


Figure 2: Effect of the loss of one ancilla qubit on the QFI for the depolarizing channel. Top plot: dotted line: optimal strategy / GHZ with no loss; 1-dash line: W-2 with no loss; 2-dash line: W-2 with one lost; 3-dash line: W-5 with no loss; 4-dash line: W-5 with one lost; full line: separable scheme / GHZ with one qubit lost. Bottom plot ($p = 0.2$): full circles: GHZ with no loss; diamonds: W states with no loss; triangle up: W states with one ancilla lost; squares: separable scheme / GHZ with one ancilla lost.

4.2.2 W states

After propagation of a W state through the extended depolarizing channel and the subsequent loss of an ancilla qubit, the state of the system

$$\begin{aligned} \rho_{\text{dep},1}^{W-n} &\equiv \text{Tr}_1 \left[\mathcal{E}_{\text{dep}}^{(n)}(\rho^{W-n}) \right] \\ &= \frac{1}{n+1} (|0, 0_{n-1}\rangle\langle 0, 0_{n-1}| + |1_1\rangle\langle 1_1|) \\ &\quad + \frac{2-p}{2(n+1)} \sum_{i,j=2}^n |1_i\rangle\langle 1_j| + \frac{1-p}{n+1} \sum_{i=2}^n (|1_1\rangle\langle 1_i| \\ &\quad + |1_i\rangle\langle 1_1|) + \frac{p}{2(n+1)} \sum_{i,j=2}^n |1, 1_i\rangle\langle 1, 1_j|, \end{aligned} \quad (46)$$

has a block structure with three non-vanishing blocks:

- a first non-contributing 1×1 block composed by the eigenvalue $\frac{1}{n+1}$.
- a second block $G^{(n-1)}(a)$ with $a = \frac{p}{2(n+1)}$.

- a third block $K^{(n)}(a, b, c)$ with $a = \frac{2-p}{2(n+1)}$, $b = \frac{1-p}{n+1}$ and $c = \frac{1}{n+1}$.

This leads to

$$I_{\text{dep},1}^{W-n} = \frac{n-1}{n+1} \frac{n(2p-3)-9}{p(2p-3)(2n-p(n-1))}. \quad (47)$$

We show in Fig. 2 the effect of the loss of one ancilla when estimating the depolarizing channel. In the top plot the QFI is represented as a function of p for GHZ states with and without loss, and also for W-2 and W-5 with and without loss. We see that although W-2 is more efficient than W-5 in the ideal case, when one qubit is lost W-5 fairs better than W-2. In the bottom plot we represent the QFI as a function of the number of initial ancillas. We see that by increasing n the two curves representing the W states with one ancilla lost and the W states without loss converge to the QFI achieved with the separable strategy.

4.3 Phase-flip channel

We now turn our attention to the phase-flip channel. For the GHZ state we have $\rho_{\text{ph},1}^{\text{GHZ}-n} \equiv \text{Tr}_1 \left[\mathcal{E}_{\text{ph}}^{(n)}(\rho^{\text{GHZ}-n}) \right] = \mathcal{E}_{\text{ph}}^{(n-1)}(\rho_1^{\text{GHZ}-n})$. But the mixed state $\rho_1^{\text{GHZ}-n}$ is a stationary state of $\mathcal{E}_{\text{ph}}^{(n-1)}$, and thus there is nothing to estimate, $I_{\text{ph},1}^{\text{GHZ}-n} = 0$.

For the W state the state of the system is $\rho_{\text{ph},1}^{W-n} \equiv \text{Tr}_1 \left[\mathcal{E}_{\text{ph}}^{(n)}(\rho^{W-n}) \right] = \mathcal{E}_{\text{ph}}^{(n-1)}(\text{Tr}_1 [\rho^{W-n}])$. Direct calculation gives

$$\rho_{\text{ph},1}^{W-n} = \frac{1}{n+1} |0, 0_{n-1}\rangle\langle 0, 0_{n-1}| + \frac{n}{n+1} \rho_{\text{ph}}^{W-(n-1)}. \quad (48)$$

Note that $\rho_{\text{ph},1}^{W-n}$ can be written as a direct sum. Since the first block does not depend on p , we can compute the QFI directly from the second block,

$$I_{\text{ph},1}^{W-n} = \frac{n}{n+1} I_{\text{ph}}^{W-(n-1)} = \frac{4(n-1)}{n(n+1)} \frac{1}{p(1-p)}. \quad (49)$$

We see in the top plot of Fig. 3 that this time W-2 has a larger QFI than W-5 with *and without loss*. In the bottom plot we observe the convergence of the QFI to zero for the W states in the ideal case and with one ancilla lost.

5 Generalization to the loss of l ancillas

Now we consider the situation where we lose l ancillas, $1 \leq l \leq n$. Since this loss channel acts only on the ancilla space it commutes with the channel acting on the

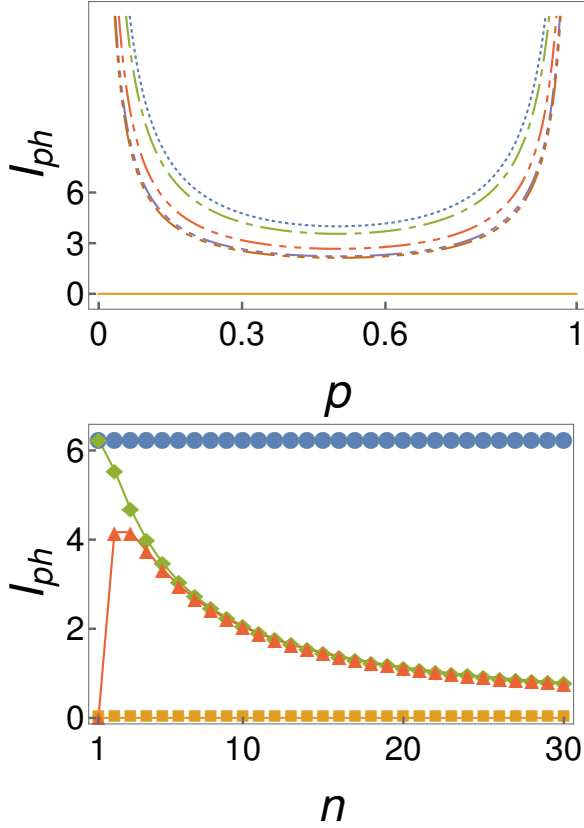


Figure 3: Effect of the loss of one ancilla qubit on the QFI for the phase-flip channel. Top plot: dotted line: GHZ with no loss / optimal separable scheme; 1-dash line: W-2 with no loss; 2-dash line: W-2 with one qubit lost; 3-dash line: W-5 with no loss; 4-dash line: W-5 with one qubit lost; full line: GHZ with one qubit lost. Bottom plot ($p = 0.2$): full circles: GHZ with no loss / optimal separable scheme; diamonds: W states with no loss; triangle up: W states with one ancilla lost; squares: GHZ with one ancilla lost.

probe, and the situation is equivalent to starting with a state which underwent already the loss of the ancillas.

5.1 Depolarizing channel

5.1.1 GHZ states

When one starts with a GHZ state and loses l qubits, the state becomes

$$\text{Tr}_l [\rho^{\text{GHZ},n}] = (|0, 0_{n-l}\rangle\langle 0, 0_{n-l}| + |1, 1_{n-l}\rangle\langle 1, 1_{n-l}|) / 2. \quad (50)$$

Losing one ancilla or $l \geq 2$ ancillas makes no difference for the QFI. Indeed the GHZ state is so sensitive to loss of particles that losing one qubit or more always leads to a mixed state of the same form (see Sec.1). We thus have for

the depolarizing channel and $1 \leq l \leq n-1$

$$I_{\text{dep},l}^{\text{GHZ},n} = I_{\text{dep}}^{\text{sep}} = \frac{1}{p(2-p)}, \quad (51)$$

and for $n = l$

$$I_{\text{dep},l}^{\text{GHZ},l} = 0. \quad (52)$$

5.1.2 W states

For the W state, the situation is substantially different since the form of the state depends on the number of lost ancillas:

$$\rho_l^{\text{W},n} = \text{Tr}_l [\rho^{\text{W},n}] = \frac{l}{n+1} |0, 0_{n-l}\rangle\langle 0, 0_{n-l}| + \frac{n+1-l}{n+1} \rho^{\text{W},(n-l)}. \quad (53)$$

For the depolarizing channel, the state

$$\begin{aligned} \rho_{\text{dep},l}^{\text{W},n} &\equiv \text{Tr}_l [\rho_{\text{dep}}^{\text{W},n}] \\ &= \frac{2l-p(l-1)}{2(n+1)} |0, 0_{n-1}\rangle\langle 0, 0_{n-1}| \\ &\quad + \frac{2+p(l-1)}{2(n+1)} |1_1\rangle\langle 1_1| + \frac{2-p}{2(n+1)} \sum_{i,j=2}^{n+1-l} |1_i\rangle\langle 1_j| \\ &\quad + \frac{1-p}{n+1} \sum_{i=2}^{n+1-l} (|1_i\rangle\langle 1_i| + |1_i\rangle\langle 1_1|) \\ &\quad + \frac{p}{2(n+1)} \sum_{i,j=2}^{n+1-l} |1, 1_i\rangle\langle 1, 1_j|, \end{aligned} \quad (54)$$

has three non-vanishing blocks:

- a first 1×1 block composed by the eigenvalue $\frac{2l-p(l-1)}{2(n+1)}$.
- a second block $G^{(n-l)}(a)$ with $a = \frac{p}{2(n+1)}$.
- a third block $K^{(n+1-l)}(a, b, c)$ with $a = \frac{2-p}{2(n+1)}$, $b = \frac{1-p}{n+1}$ and $c = \frac{2+p(l-1)}{2(n+1)}$.

They lead to the QFI

$$\begin{aligned} I_{\text{dep},l}^{\text{W},n} &= \left\{ -2p \left(-2(l(l+2)-1)n^2 + l(l(3l+2)-9)n \right. \right. \\ &\quad \left. \left. + l(l(3l+4)-9) + 8n+2 \right) + (l-1)(l+3)(n+1)p^2(2l-n-1) \right. \\ &\quad \left. + 4l(l+2)(n+3)(l-n) \right\} / \left\{ (n+1)p((l-1)p-2l) \right. \\ &\quad \left. ((l+3)p-2(l+2))(l(2-2p)+(n+1)(p-2)) \right\}. \end{aligned} \quad (55)$$

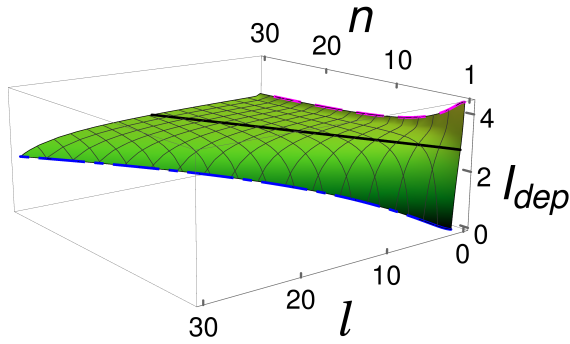


Figure 4: QFI for the depolarizing channel for a W state with n ancillas and l lost ones ($p = 0.2$). The full line corresponds to the separable strategy or GHZ with loss, the dashed line to the case where no ancillas are lost ($l = 0$) and the 1-dash line to the case where all ancillas are lost ($l = n$).

One checks that by setting l to zero or to one we recover our previous results (31) and (47), respectively. In terms of gain due to extension, we can calculate the number of lost ancillas as a function of the number of initial ancillas such that the scheme stays more efficient than the separable strategy. This function is cumbersome but actually behaves mainly linearly with a slope of 0.5. This means that when more than half the ancillas are lost, the strategy of using W states becomes less efficient than the separable strategy. But for depolarizing channel, this strategy is equivalent to the use of a GHZ state with some ancillas lost (45,51). Thus this bound gives us also the value of l as a function of n for which it is worth to start with a GHZ state rather than with a W state. This is visualized in Fig. 4, representing the QFI for the depolarizing channel as a function of n and l , and where the full black line represents the QFI for the separable strategy or GHZ with loss.

In Fig. 5 we demonstrate the effect of the loss on the estimation of the depolarizing channel. In the top plot we show the QFI as a function of p . We plot the optimal result (dotted line) and the separable strategy (full line). The different dash lines show W-8 with either no loss, or two, or six ancillas lost. In agreement with the bound discussed in the previous paragraph, for six ancillas lost in W-8, the protocol is less efficient than the separable one / GHZ with loss. In the bottom plot we show the QFI for the depolarizing channel as a function of the number of lost ancillas. We observe that W states with a larger number of ancillas are more resistant to the loss of qubits, but have a lower initial QFI. There is a compromise for the optimal choice

of n in a W state between initial QFI and robustness to the loss. When the number of lost ancillas equals roughly half the number of initial ancillas, the W states become less efficient than the GHZ states (this is more clear in the subplot). When all the ancillas are lost, the QFI still not vanishes, provided that $n > 1$: Setting l to n in eq.(55), leads to

$$I_{\text{dep},n}^{W-n} = \frac{(n-1)^2}{(2+(n-1)p)(p+n(2-p))}, \quad (56)$$

which converges to $I_{\text{dep}}^{\text{sep}}$ when n goes to infinity. For $n = 1$, $I_{\text{dep},1}^{W-1} = 0$.

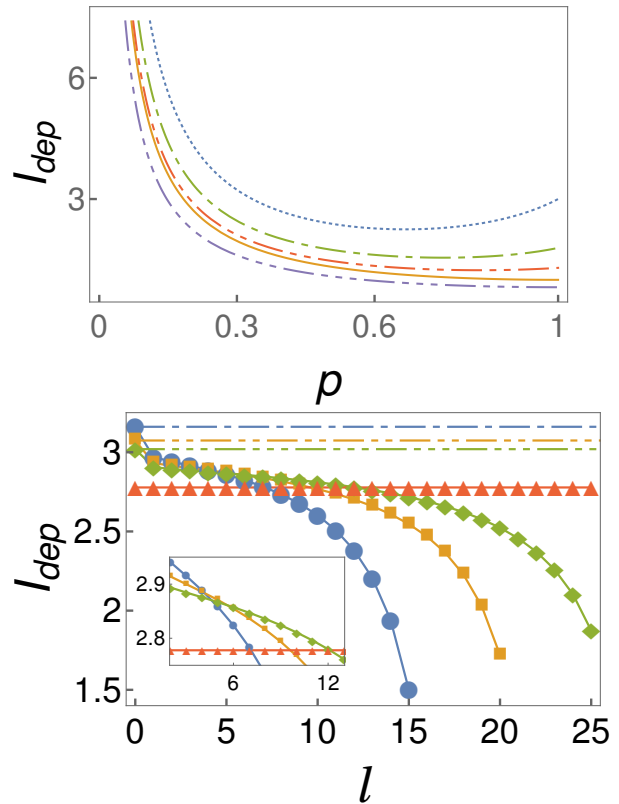


Figure 5: QFI for depolarizing channel for arbitrary loss. Top plot: dotted line: GHZ with no loss; 1-dash line: W-8 with no loss; 2-dash line: W-8 with 2 lost; 3-dash line: W-8 with 6 lost; full line: separable strategy / GHZ with one lost. Bottom plot ($p = 0.2$): 1-dash line: W-15 with no loss; full circles: W-15 with loss; 2-dash line: W-20 with no loss; squares: W-20 with loss; 3-dash line: W-25 with no loss; diamonds: W-25 with loss; triangle up: separable strategy / GHZ with one lost.

5.2 Phase flip channel

Again, for the sake of comparison, we give a brief look at the phase-flip channel. For the GHZ states and $1 \leq l \leq n$

the QFI vanishes,

$$I_{\text{ph},l}^{\text{GHZ},n} = 0. \quad (57)$$

In the case of the phase-flip channel, the state (53) after application of the channel and loss of l ancillas has the form of a direct sum involving a known state, leading to the QFI

$$I_{\text{ph},l}^{W,n} = \frac{n+1-l}{n+1} I_{\text{ph}}^{W-(n-l)} = \frac{4(n-l)}{(n+1)(n+1-l)} \frac{1}{p(1-p)}. \quad (58)$$

As expected, the QFI decreases as function of l : The more ancillas are lost the worse is the estimation. When all ancillas are lost the QFI vanishes, since the resulting state is insensitive to the phase-flip channel.

This is demonstrated in Fig. 6. The top plot shows the QFI as a function of p . In the bottom plot $p = 0.2$, and we plot the QFI as a function of the number of lost ancillas for W states. The more ancillas we add the smaller the initial QFI, but also the QFI decreases more slowly as function of l . This leads to an optimal number of initial ancillas for a given number of ancillas lost, even though we have to remember that for the phase-flip channel the best strategy is to not use any ancillas at all (see Sec.2.5).

5.3 Gain versus robustness

There is a competition between the initial value of the QFI and the robustness for W states for both channels (although for the phase-flip channel we know that the optimal scheme is the non-extended one).

For the depolarizing channel, when looking at the bottom plot in Fig. 5, we see that while in the ideal case ($l = 0$) $W-15$ is more efficient than $W-25$, this is already no longer true when six ancillas are lost as the inset clearly shows. More generally there exists for a given fixed number l of ancillas lost an optimal number $n_{\text{opt,dep}}(l)$ of initial ancillas in the W state, see top plot of Fig. 7. The function $n_{\text{opt,dep}}(l)$ has a complicated form, but its leading term is given by

$$n_{\text{opt,dep}}(l) \simeq \left(2 + \frac{2}{\sqrt{2-p}} \right) l, \quad (59)$$

which for $p = 0.2$ gives roughly $3.5l$. We see that this is in good agreement with the inset of the top plot of Fig. 7. Nevertheless, when increasing the number of ancillas in the W state we get a QFI closer to the one of the separable strategy, and thus the small gain in QFI may not justify the use of so many ancillas. As an example, when losing fifteen ancillas, the best W state is $W-55$ (the leading term in this case will give $n_{\text{opt,dep}} = 52$ or 53), but its QFI equals 2.81 and the QFI for the separable strategy equals 2.77.

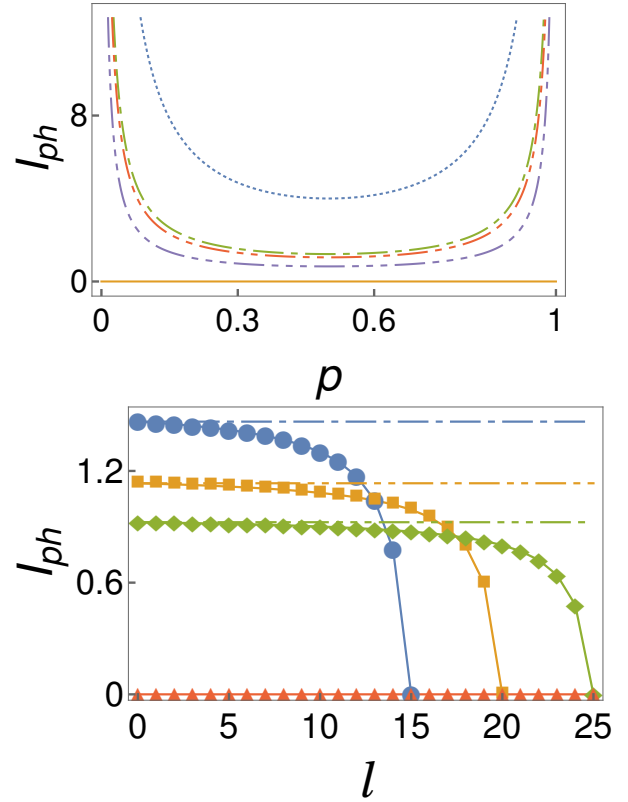


Figure 6: QFI for phase-flip channel for arbitrary loss. Top plot: dotted line: optimal strategy / GHZ with no loss; 1-dash line: $W-10$ with no loss; 2-dash line: $W-10$ with 6 lost; 3-dash line: $W-10$ with 9 lost; full line: GHZ with at least one ancilla lost. Bottom plot ($p = 0.2$): 1-dash line: $W-15$ with no loss; full circles: $W-15$ with loss; 2-dash line: $W-20$ with no loss; squares: $W-20$ with loss; 3-dash line: $W-25$ with no loss; diamonds: $W-25$ with loss; triangle up: GHZ with loss (GHZ without loss is not represented).

A similar behavior is observed for the phase-flip channel. Although there the optimal strategy consists to not add any ancilla, the study of the QFI for a fixed number of lost ancillas leads also to a maximum as represented in the bottom plot in Fig. 7. We can here too calculate the optimal number of initial ancillas as a function of lost ancillas in a W state

$$n_{\text{opt,ph}}(l) = \begin{cases} \lfloor l + \sqrt{1+l} \rfloor \equiv l_f & \text{if } I_{\text{ph},l}^{W-l_f} > I_{\text{ph},l}^{W-l_c}, \\ \lceil l + \sqrt{1+l} \rceil \equiv l_c & \text{if } I_{\text{ph},l}^{W-l_f} < I_{\text{ph},l}^{W-l_c}, \\ \{l_f, l_c\} & \text{if } I_{\text{ph},l}^{W-l_f} = I_{\text{ph},l}^{W-l_c}, \end{cases} \quad (60)$$

with $\lfloor \cdot \rfloor$ the floor function and $\lceil \cdot \rceil$ the ceiling function. Thus $n_{\text{opt,ph}}$ scales roughly linearly with l .

Table 1: Summary for the depolarizing channel

State	Benchmark	State	Ideal case	l ancillas lost
Maximally entangled	Optimal: $I_{\text{dep}}^{\text{opt}} = \frac{3}{p(4-3p)}$.	GHZ (n ancillas)	Still optimal.	$l \geq 1$: goes back to separable. $l = n$: QFI vanishes.
Separable (pure state)	$I_{\text{dep}}^{\text{sep}} = \frac{1}{p(2-p)}$ (independent of the state).	W (n ancillas)	Decreases with n . In between optimal and separable.	Exists an optimal n for a given l . Adding ancillas can protect the QFI.

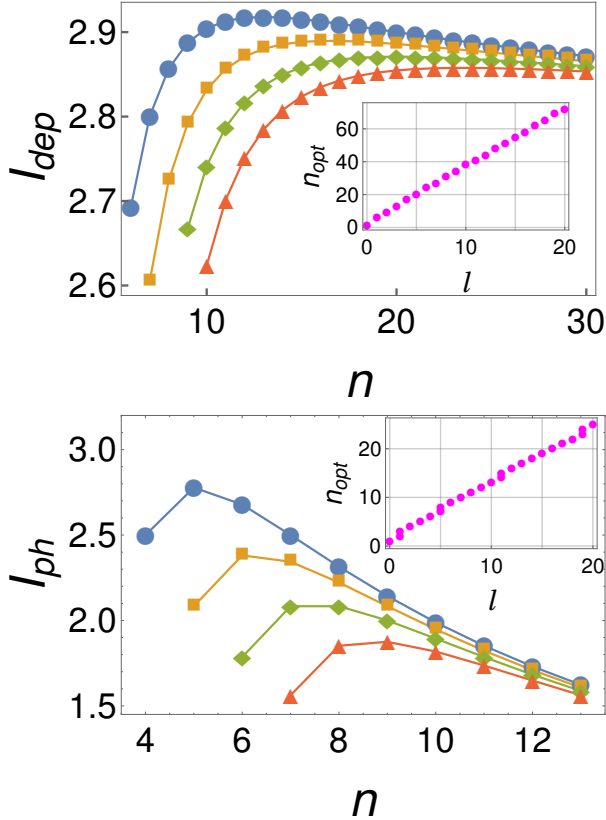


Figure 7: Main plots: QFI as a function of the number of initial ancillas in a W state for a fixed number of lost ancillas. The full circles correspond to three ancillas lost, the squares to four, the diamonds to five, and the triangle to six. In the insets we see the optimal number of initial ancillas in a W state as a function of the number of lost ancillas. The top plot corresponds to the depolarizing channel, the bottom one to the phase-flip channel ($p = 0.2$).

6 Conclusions

We investigated the robustness of channel estimation schemes for depolarizing and phase-flip channels of qubits extended to ancilla qubits, when one or several of the qubits can get lost. Without loss of qubits, the optimal estimation strategy consists for both channels in extending the channel by a single ancilla qubit that remains un-

touched, but feeding the whole channel with a maximally entangled state [20].

For the depolarizing channel this leads, when no qubit is lost, to a real improvement compared to the non-extended case. For the phase-flip channel the maximum quantum Fisher information (QFI) can also be achieved with a non-extended channel fed with a specific pure state, showing that no extension is necessary. We extended this investigation to the case where an arbitrary number of qubits can be added or lost, including the original probe qubit. We used GHZ and W states as input states for the channels.

For the GHZ states, the QFI in the absence of loss is equal to the optimal one for both channels, independently of the number of ancillas. In the presence of loss, for the depolarizing channel and provided that not all the ancillas are lost — in which case the QFI vanishes —, the QFI is independent of the number of lost ancillas and equals the one of the non-extended case. For the phase-flip channel the loss of already one ancilla leads to a vanishing QFI.

For the W states, the QFI for the depolarizing channel without loss decreases with the number of added ancillas. While for one ancilla we are in the optimal case, when the number of ancillas goes to infinity the QFI goes to the QFI of the separable strategy. The interesting point lies in the fact that the W states are more resistant to loss, as for a fixed number of lost ancillas, there always exists a W state with larger QFI after the loss of these ancillas than the one of the separable strategy. In this sense the W states, although not optimal without loss of qubits, can lead to a better estimation in non-ideal situations for the depolarizing channel. We summarized the main results for depolarizing channel in the table 1. The resistance to loss is also observed in the phase-flip channel, but does not lead to any improvement in estimation, since it is still better to not add ancillas at all.

Acknowledgement: We gratefully acknowledge useful correspondence with A. Fujiwara. We thank Matteo Paris and Hossein Rangani for discussions and correspondence.

A Appendix: decomposition of matrices

In order to calculate the QFI we need to diagonalize the density matrix. For the states in which we are interested, there are two matrices $K^{(m)}(a, b, c)$ and $G^{(m)}(a)$ that recurrently appear in the block decomposition of the states:

- The $m \times m$ matrix $K^{(m)}(a, b, c)$:

$$K^{(m)}(a, b, c) = \begin{pmatrix} a & \cdots & a & b \\ \vdots & \ddots & \vdots & \vdots \\ a & \cdots & a & b \\ b & \cdots & b & c \end{pmatrix}. \quad (61)$$

This matrix has rank two, the two non-zero eigenvalues

$$\lambda_{\pm}^{(K)} = \frac{1}{2} \left(c + a(m-1) \pm \sqrt{(c - a(m-1))^2 + 4b^2(m-1)} \right), \quad (62)$$

and the two corresponding non-normalized eigenvectors

$$\mathbf{v}_{\pm}^{(K)} = (2b, \dots, 2b, Y_{\pm}^{(K)}), \quad (63)$$

with $Y_{\pm}^{(K)} = c - a(m-1) \pm \sqrt{(c - a(m-1))^2 + 4b^2(m-1)}$.

- The $m \times m$ matrix $G^{(m)}(a)$:

$$G^{(m)}(a) = \begin{pmatrix} a & \cdots & a \\ \vdots & \ddots & \vdots \\ a & \cdots & a \end{pmatrix}, \quad (64)$$

which only non-zero eigenvalue is

$$\lambda^{(G,m)} = ma, \quad (65)$$

and the non-normalized corresponding eigenvector is

$$\mathbf{v}^{(G,m)}(a) = (1, \dots, 1). \quad (66)$$

References

- [1] Mehdi Ahmadi, David Edward Bruschi, Carlos Sabín, Gerardo Adesso, and Ivette Fuentes. Relativistic quantum metrology: Exploiting relativity to improve quantum measurement technologies. *Sci. Rep.*, 4, May 2014.
- [2] F. Benatti and D. Braun. Sub-shot-noise sensitivities without entanglement. *Phys. Rev. A*, 87:012340, Jan 2013.
- [3] Ingemar Bengtsson and Karol Życzkowski. *Geometry of quantum states: an introduction to quantum entanglement*. Cambridge University Press, 2006.
- [4] D. Braun. Ultimate quantum bounds on mass measurements with a nano-mechanical resonator. *Europhys. Lett.*, 94(6):68007, 2011.
- [5] Daniel Braun. Ultimate quantum bounds on mass measurements with a nano-mechanical resonator. *EPL*, 99(4):49901, August 2012.
- [6] Daniel Braun, Olivier Giraud, Ion Nechita, Clément Pellegrini, and Marko Žnidarič. A universal set of qubit quantum channels. *Journal of Physics A: Mathematical and Theoretical*, 47(13):135302, April 2014.
- [7] Daniel Braun, Fabienne Schneiter, and Uwe R. Fischer. How precisely can the speed of light be determined? *arXiv:1502.04979 [gr-qc, physics:quant-ph]*, February 2015. arXiv: 1502.04979.
- [8] Samuel L. Braunstein and Carlton M. Caves. Statistical distance and the geometry of quantum states. *Phys. Rev. Lett.*, 72:3439–3443, May 1994.
- [9] Samuel L. Braunstein, Carlton M. Caves, and G. J. Milburn. Generalized uncertainty relations: Theory, examples, and lorentz invariance. *Annals of Physics*, 247(1):135–173, April 1996.
- [10] Samuel L. Braunstein and G. J. Milburn. Dynamics of statistical distance: Quantum limits for two-level clocks. *Phys. Rev. A*, 51(3):1820–1826, Mar 1995.
- [11] David Collins. Mixed-state Pauli-channel parameter estimation. *Physical Review A*, 87(3), March 2013.
- [12] David Collins and Jaimie Stephens. Depolarizing-channel parameter estimation using noisy initial states. *Phys. Rev. A*, 92:032324, Sep 2015.
- [13] Luis A. Correa, Mohammad Mehboudi, Gerardo Adesso, and Anna Sanpera. Individual quantum probes for optimal thermometry. *Phys. Rev. Lett.*, 114:220405, Jun 2015.
- [14] H. Cramér. *Mathematical Methods of Statistics*. Princeton University Press, Princeton, NJ, 1946.
- [15] Philip J. D. Crowley, Animesh Datta, Marco Barbieri, and I. A. Walmsley. Tradeoff in simultaneous quantum-limited phase and loss estimation in interferometry. *Physical Review A*, 89(2), February 2014.
- [16] Julien Mathieu Elias Fraïsse and Daniel Braun. Coherent averaging. *Annalen der Physik*, pages 1–12, July 2015.
- [17] Michael Frey, David Collins, and Karl Gerlach. Probing the qudit depolarizing channel. *Journal of Physics A: Mathematical and Theoretical*, 44(20):205306, 2011.
- [18] Akio Fujiwara. Quantum channel identification problem. *Physical Review A*, 63(4), March 2001.
- [19] Akio Fujiwara and Paul Algoet. One-to-one parametrization of quantum channels. *Phys. Rev. A*, 59:3290–3294, May 1999.
- [20] Akio Fujiwara and Hiroshi Imai. Quantum parameter estimation of a generalized Pauli channel. *Journal of Physics A: Mathematical and General*, 36(29):8093, 2003.
- [21] V. Giovannetti, S. Lloyd, and L. Maccone. Quantum metrology. *Physical Review Letters*, 96(1):010401, 2006.
- [22] C. Gross, T. Zibold, E. Nicklas, J. Estève, and M. K. Oberthaler. Nonlinear atom interferometer surpasses classical precision limit. *Nature*, 464(7292):1165–1169, 04 2010.
- [23] C. W. Helstrom. Quantum detection and estimation theory. *Journal of Statistical Physics*, 1(2):231–252, 1969.
- [24] A. S. Holevo. *Probabilistic and Statistical Aspect of Quantum Theory*. North-Holland, Amsterdam, 1982.
- [25] A. S. Holevo. *Statistical Structure of Quantum Theory*, volume 61 of *Lect. Not. Phys.* Springer, Berlin, 2001.

- [26] M. J. Holland and K. Burnett. Interferometric detection of optical phase shifts at the heisenberg limit. *Phys. Rev. Lett.*, 71:1355–1358, Aug 1993.
- [27] S. F. Huelga, C. Macchiavello, T. Pellizzari, A. K. Ekert, M. B. Plenio, and J. I. Cirac. Improvement of frequency standards with quantum entanglement. *Phys. Rev. Lett.*, 79(20):3865–3868, 1997.
- [28] S. F. Huelga, C. Macchiavello, T. Pellizzari, A. K. Ekert, M. B. Plenio, and J. I. Cirac. Improvement of frequency standards with quantum entanglement. *Phys. Rev. Lett.*, 79(20):3865–3868, 1997.
- [29] J. Aasi, *et al.* Enhanced sensitivity of the LIGO gravitational wave detector by using squeezed states of light. *Nat Photon*, 7(8):613–619, 08 2013.
- [30] K. Kraus. *States, Effects and Operations, Fundamental Notions of Quantum Theory*. Academic, Berlin, 1983.
- [31] Alfredo Luis. Nonlinear transformations and the heisenberg limit. *Phys. Lett. A*, 329(1-2):8–13, August 2004.
- [32] Ugo Marzolino and Daniel Braun. Precision measurements of temperature and chemical potential of quantum gases. *Phys. Rev. A*, 88(6):063609, December 2013.
- [33] M. Mehboudi, M. Moreno-Cardone, G. De Chiara, and A. Sanpera. Thermometry precision in strongly correlated ultracold lattice gases. *New J. Phys.*, 17:055020, 2015.
- [34] J. A. Miszczak, Z. Puchała, P. Horodecki, A. Uhlmann, and K. Życzkowski. Sub- and super-fidelity as bounds for quantum fidelity. *Quantum Information and Computation*, 9:0103, 2009.
- [35] M Napolitano and M W Mitchell. Nonlinear metrology with a quantum interface. *New J. Phys.*, 12(9):093016, 2010.
- [36] Michael A. Nielsen and Isaac L. Chuang. *Quantum Computation and Quantum Information: 10th Anniversary Edition*. Cambridge University Press, New York, NY, USA, 10th edition, 2011.
- [37] M. G. A. Paris. Quantum estimation for quantum technology. *International Journal of Quantum Information*, 7:125, 2009.
- [38] A. Peres. *Quantum Theory: Concepts and Methods*. Kluwer Academic Publishers, Dordrecht, 1993.
- [39] Dénes Petz. Monotone metrics on matrix spaces. *Linear Algebra and its Applications*, 244:81–96, September 1996.
- [40] John Preskill. Lecture notes for ph219/cs219: Quantum information chapter 3, July 2015.
- [41] C. Rao. Information and the accuracy attainable in the estimation of statistical parameters. *Bulletin of the Calcutta Mathematical Society*, 37:81, 1945.
- [42] Thomas M. Stace. Quantum limits of thermometry. *Phys. Rev. A*, 82:011611, Jul 2010.
- [43] Magdalena Szczykulska, Tillmann Baumgratz, and Animesh Datta. Multi-parameter quantum metrology. *Advances in Physics: X*, 1(4):621–639, 2016.
- [44] Alexandre B. Tacla, Sergio Boixo, Animesh Datta, Anil Shaji, and Carlton M. Caves. Nonlinear interferometry with bose-einstein condensates. *Phys. Rev. A*, 82:053636, Nov 2010.
- [45] Mihai D. Vidrighin, Gaia Donati, Marco G. Genoni, Xian-Min Jin, W. Steven Kolthammer, M.S. Kim, Animesh Datta, Marco Barbieri, and Ian A. Walmsley. Joint estimation of phase and phase diffusion for quantum metrology. *Nature Communications*, 5, April 2014.
- [46] Y. M. Zhang, X. W. Li, W. Yang, and G. R. Jin. Quantum Fisher information of entangled coherent states in the presence of photon loss. *Phys. Rev. A*, 88(4):043832, October 2013.